Clinical and radiological findings of glioblastomas harboring a BRAF V600E mutation

Yukitomo Ishi [1]

Shigeru Yamaguchi[1]

Michinari Okamoto [1]

Ryosuke Sawaya[1]

Shogo Endo [2]

Hiroaki Motegi[1]

Shunsuke Terasaka [3]

Zen-ichi Tanei [4]

Kanako C. Hatanaka[5]

Shinya Tanaka [4,6]

Miki Fujimura [1]

[1]Department of Neurosurgery, Hokkaido University School of Medicine, North 15 West 7, Kita-ku, Sapporo 060-8638, Japan

[2]Department of Neurosurgery, Hokkaido Neurosurgical Memorial Hospital, 1-20, Hachiken 9-jo, Higashi 5-chome, Nishi-ku, Sapporo 063-0869, Japan.

[3]Department of Neurosurgery, Kashiwaba Neurosurgical Hospital, 7-20, East 1-15 Tsukisamu, Toyohira-ku, Sapporo 062-8513, Japan.

[4]Department of Cancer Pathology, Hokkaido University School of Medicine, North 15 West 7, Kita-ku, Sapporo 060-8638, Japan

[5]Department of Surgical Pathology, Hokkaido University Hospital, North 14 West 4, Kita-ku, Sapporo 060-8648, Japan

[6]WPI-ICReDD, Hokkaido University, North 15 West 7, Kita-ku, Sapporo 060-8638, Japan

Corresponding Author:

Shigeru Yamaguchi,

Department of Neurosurgery

Hokkaido University Graduate School of Medicine

North 15 West 7, Kita-ku, Sapporo 060-8638, Japan

Phone: (+81)11-706-5987

Fax: (+81)11-708-7737

E-mail: yama-shu@med.hokudai.ac.jp

Total word count: 4592

Abstract

The aim of this study was to analyze the clinical and radiological characteristics of glioblastomas (GBMs) harboring a *BRAF* mutation. Sequencing analysis of *BRAF*, *IDH1/2*, and *TERT* promoters was performed on GBM samples of patients older than 15 years. The clinical, pathological, and radiological data of patients were retrospectively reviewed. Patients were classified into three groups according to their *BRAF* and *IDH1/2* status: BRAF group, IDH group, and BRAF/IDH-wild-type (WT) group. Among 179 GBM cases, we identified nine cases with a *BRAF* mutation and nine with IDH mutation. The WT group had 161 cases. Age at onset in the BRAF group was significantly lower compared to the WT group and was similar to the IDH group. In cases with negative IDH1-R132H staining and age <55 years, 15.2% were *BRAF*-mutant cases. Similar to the IDH group, overall survival of the BRAF group was significantly longer compared with the WT group. Among nine cases in the BRAF group, three cases had hemorrhagic onset and prior lesions were observed in two cases. In conclusion, Age <55 years, being IDH1-R132H negative, with hemorrhagic onset or the presence of prior lesions are factors that signal recommendation of *BRAF* analysis for adult GBM patients.

(198/200 words)

KEYWORDS: *BRAF* V600E; glioblastoma; *IDH1/2*; MRI

Introduction

The World Health Organization (WHO) classification of central nervous tumors, revised in 2016, classified glioblastoma (GBM) into two groups according to the genetic status of *isocitrate dehydrogenase* (*IDH*); that is, GBM-*IDH* mutant, and GBM-*IDH* wild-type (WT) [1]. In the 2021 WHO classification, *IDH*-mutant cases were classified as "astrocytoma, *IDH*-mutant grade 4," and *IDH*-wild cases as "GBM, *IDH*-WT" [2]. Due to the poor prognosis of GBM despite standardized treatment with temozolomide (TMZ) and radiotherapy (RT), further molecular therapies targeting genetic alterations in GBMs have been explored [3].

A missense mutation at the amino acid position 600 of the *Braf proto-oncogene* (*BRAF* V600E) is frequently detected in pediatric low-grade gliomas, including 18%–38.7% of gangliogliomas [4-6], 9%–15.6% of pilocytic astrocytomas [4-6], and 50%–66.7% of pleomorphic xanthoastrocytomas (PXAs) [4-7]. The *BRAF* mutation has been detected in a subset of GBMs [6, 8-11] and the majority of epithelioid GBMs (E-GBMs), which is an aggressive subtype of GBM [12, 13]. E-GBM has been described as a variant of GBM in the WHO classification in 2016 [1], and a histological pattern of "glioblastoma, IDH-wildtype" in the WHO classification in 2021[14]. Regarding the molecular features of GBM with the *BRAF* mutation (*BRAF*-GBM), recent studies have revealed that a missense mutation in the promoter of *telomerase reverse transcriptase* (*TERT*) and homozygous deletion of *cyclin-dependent kinase inhibitor 2A* (*CDKN2A*-HD) were frequent and similar to *IDH*-wild GBMs [13, 15]. However, the clinical features of *BRAF*-GBM have not been elucidated due to the low number of cases.

The efficacy of targeting therapy for *BRAF* V600E using dabrafenib and trametinib have been reported in clinical experiences [16-25]. To screen the potential targeting therapy candidates for *BRAF* V600E, clinical sequencing of cancer-associated genes would be the most appropriate approach in clinical practice [26]. However, there are no standardized principles to recommend clinical sequencing in GBM patients, and the clinical characteristics of *BRAF*-GBM would have significant value for recommendation of *BRAF* screening. The aim of this study was to reveal the clinical and radiological features of *BRAF*-GBM.

Methods

Patient population

This study included patients with GBM who underwent treatment in Hokkaido University Hospital from 2000 to 2021 and whose frozen tumor tissues were available. Adult and young adult patients older than 15 years of age were

included. Pathological diagnoses of GBM were provided by institutional pathologists according to the WHO classification of Central Nervous System revised 4th edition in 2016 [27]. Clinical, pathological, and radiological data of patients were retrospectively analyzed by referring to their medical record. All manipulations were performed under approval from our institutional review board. As this study was retrospective, the requirement for informed consent was waived.

Genetic analysis

DNA/RNA was extracted from frozen tumor tissues using an AllPrep DNA/RNA Mini Kit (Qiagen, Tokyo, Japan) in accordance with the manufacturer's recommendations. Two hotspots within the *TERT* promoter (C228T, C250T), along with mutation hotspots at codon 132 of *IDH1*, codon 172 of *IDH2*, and codon 600 of *BRAF* were screened using Sanger sequencing, as previously described [28]. *CDKN2A*-HD was analyzed by multiplex ligation-dependent probe amplification [8], or we referred to the result of the clinical sequencing panel using FoundationOne® CDx (Foundation Medicine, Cambridge, USA) or OncoGuide™ (Sysmex, Kobe, Japan).

Statistical analysis

Statistical analysis was performed using Graphpad Prism 8 (GraphPad Software, San Diego, CA). A p value less than 0.05 was considered statistically significant for a log-rank test and analysis of variance (ANOVA) with a Tukey-Kramer test as a post hoc analysis.

Results

Patient demographics

Among the 179 cases analyzed in this study, mutations in *BRAF*, *IDH1/2,* and *TERT* promoter mutations were detected in 9 cases (5.0%), 9 cases (5.0%) and 96 cases (54.9%), respectively (Fig. 1a). None of the *BRAF*-mutant cases presented co-occurrence with the *IDH* mutation and one case with the *BRAF* mutation presented co-occurrence with the *TERT* promoter mutation. Pathological diagnoses in *BRAF*-mutant cases were classical GBM in eight cases and epithelioid GBM in one case. Eight of nine cases had a *BRAF* V600E mutation and one case had an in-frameshift deletion with *BRAF* c.1799_1801del that resulted in p.V600E and p.K601del. *CDKN2A*-HD was detected in seven cases (Table). In this study, we classified the cases into three groups according to the status of *BRAF* and *IDH1/2*: *BRAF*-

mutant (BRAF group, 9 cases), *IDH1/2*-mutant (IDH group, 9 cases), and wild-type *BRAF* and *IDH1/2* (WT group, 161 cases).

Clinical characteristics of GBM with the *BRAF mutation*

Clinical features of nine cases with the *BRAF* mutation, including eight cases with classical GBM and one case with E-GBM, are summarized in Table. The median age at onset of the *BRAF* group was 37 years (range 27–66), which was significantly younger than the WT group but was similar to the IDH group (Fig. 1b). Among 46 cases with negative IDH1-R132H staining and age <55 years, seven cases with a *BRAF*-mutant accounted for 15.2%, while no cases presented with the *IDH1/2* mutation (Fig. 1c). Major symptoms at onset were seizure in three patients and stroke-like symptoms due to intratumoral hemorrhage in three patients. All patients except for one case had a single lesion that arose in a cerebral hemisphere.

Treatment outcome of GBM with a BRAF mutation

Five out of nine cases with BRAF-GBM showed recurrence including dissemination in four cases during observation period (Table). The survival curve of the BRAF group within 24 months was similar to the WT group due to early death; however, the presence of patients with long-term survival resulted in significantly longer overall survival (OS) compared with the WT group (Fig. 1d). There was no significant difference between the BRAF group and IDH group, which also presented a favorable OS compared with the WT group (Fig. 1d).

Radiological findings of GBM with BRAF mutation

Among 6 cases without hemorrhagic onset, all cases showed enhanced lesions on gadolinium-enhanced (Gd-) T1 weighted imaging (WI), while 3 cases (cases 1, 4, and 6) had mild perifocal edema on T2WI or fluid attenuated inversion recovery (FLAIR) on MRI (Supplementary Figure). A well-circumscribed border on Gd-T1WI was observed in five cases (cases 1–4 and 6, cortical involvement was observed in three cases (cases 1, 2, and 6), and a large cystic component was observed in one case (case 2). Among three cases with hemorrhagic onset, two cases had a prior lesion on FLAIR that was diagnosed at 3 and 8 years before, respectively (Table).

Representative cases

Case #1 (non-hemorrhagic onset, long-term survival without recurrence)

A 27-year-old female presented with convulsive and repeated dysosmia, which was considered as partial seizures. MRI showed a mass lesion in the mesial temporal lobe, in which Gd-T1WI showed ring-like enhancement with a well-circumscribed border and cortical involvement and FLAIR showed mild perifocal edema (Fig. 2a, Supplementary Figure). Gross total removal (GTR) was achieved at tumor resection. A pathological examination indicated a necrotic area (Fig. 2b) and dense tumor cells with nuclear atypia and mitosis (Fig. 2c). The Ki-67 labeling index was 50% and the pathological diagnosis was GBM. The patient underwent oral administration of TMZ (75 mg/m^2), 60 gray (Gy) of local RT, and a subsequent maintained administration of TMZ (150 mg/m^2/four weeks). She had no neurological deficit and no recurrence for 69 months.

Case #4 (non-hemorrhagic onset, early recurrence)

A 42-year-old male presented with a grand mal seizure. MRI indicated a tumor in the right frontal lobe with ring-like enhancement and a well-circumscribed border on Gd-T1WI and mild perifocal edema on FLAIR (Fig. 2d, Supplementary Figure). GTR was achieved at tumor resection. A pathological examination identified dense tumor cells with nuclear atypia, microvascular proliferation, and necrosis (Fig. 2e). Gemistocytic tumor cells were also observed (Fig. 2f) and the pathological diagnosis was E-GBM. He underwent oral administration of TMZ (75 mg/m^2), 60 Gy of RT, and a subsequent maintained administration of TMZ. However, local recurrence and spinal dissemination were detected at three months after surgery and he died five months after surgery.

Case #7 (hemorrhagic onset)

A 44-year-old female presented with sudden onset of headache and aphasia. Head CT showed a high-density lesion on the left insula and FLAIR on MRI showed a high intensity lesion surrounding the hematoma, which suggested hemorrhagic onset of an intra-axial tumor (Fig. 3a). Emergent surgery was performed, and the pathological specimens exhibited hematoma with a small amount of diffuse astrocytoma showing the Ki-67 labeling index of 5% (Fig. 3b). Based on the postoperative MRI presenting no apparent residual lesion (Fig. 3c) and low-grade histological malignancy, the patient was carefully observed without additional treatment; however, MRI showed recurrence at nine months after surgery (Fig. 3d). She underwent additional surgery and subtotal removal was achieved. Pathological examinations

presented increased tumor cell density and nuclear atypia. The Ki-67 labeling index was 25% and the diagnosis was GBM (Fig. 3e). She underwent oral administration of TMZ (75 mg/kg) and 60 Gy of irradiation followed by 24 courses of maintained administration of TMZ. She had no apparent recurrence for 39 months after treatment.

Case #8 (hemorrhagic onset with a prior lesion)

This male patient was shown to have an intra-axial lesion on the right occipital lobe due to headache at the age of 28 years (Fig. 4a), and he was observed at another institution. At the age of 31 years, he presented with a sudden onset headache. Head CT showed a high-density lesion in the right occipital lobe, and MRI showed mild perifocal edema and heterogenous enhancement in the lesion (Fig. 4b). Emergent surgery was performed and GTR was achieved. The pathological diagnosis was GBM (Fig. 4c) and he underwent oral administration of TMZ and 60 Gy of RT followed by maintenance TMZ. However, he underwent additional resection surgery for local recurrence at 10 months after the initial surgery. Although he was treated with TMZ and bevacizumab, distant recurrence was observed seven months later. Clinical sequencing revealed *BRAF* V600E and he started combined treatment with dabrafenib and trametinib, but he died due to progression of the disease at 29 months after initial treatment.

Case #9 (hemorrhagic onset with a prior lesion)

This male patient was diagnosed in other institution with a right temporal lobe abnormality on MRI at the age of 30 years due to epilepsy (Fig. 4d); however, surgical confirmation was not performed because the patient did not consent. At the age of 38 years, he presented with sudden onset of headache. Head CT showed a high-density lesion in the right temporal lobe, FLAIR on MRI showed a high intensity lesion around the hemorrhage, and Gd-T1WI showed ring-like enhancement (Fig. 4e). Emergent surgery was performed and the pathological diagnosis was GBM (Fig. 4f). He underwent standardized treatment with TMZ and 60 Gy of irradiation, and salvage surgery for the remaining lesion was performed after irradiation. He continued TMZ maintenance without evidence of recurrence for 30 months after the initial surgery.

Discussion

Previous reports indicated that the *BRAF* mutation accounted for 1.6%–6.3% of adult GBM cases [6, 8-10] and 15 of 633 (2.4%) adult high-grade gliomas including WHO grade 3 cases [8]. The *BRAF* mutation has been observed more

frequently with 16 of 107 (15.0%) cases in the study of young adult GBM cases [11]. Our results also indicated younger ages at onset in *BRAF*-mutated cases as well as *IDH*-mutant cases, which was consistent with previous reports [29, 30]. Because of the low frequency of *IDH* mutations in the elderly, the current WHO classification recommends sequencing analysis of *IDH1/2* in cases with age <55 years if immunostaining for IDH1-R132H is negative [1]. Although cases with co-occurrence of *BRAF* and *IDH1/2* mutations have been reported [5, 12, 29], most of the *BRAF*-mutated cases did not harbor the *IDH1/2* mutation [8, 10, 11]. Thus, we consider that analysis of the *BRAF* mutation would be valuable, especially in patients who are less than 55 years old and are negative for *IDH1*-R132H as presented in our study.

Dissemination, which is frequent in E-GBM cases [13, 15], was observed in four out of five recurrent cases including one E-GBM case in this study. Classical GBM with BRAF mutation, as well as E-GBM cases, would tend to present dissemination at recurrence. Although *BRAF*-GBM tended to present favorable treatment outcomes compared to other *IDH*-wild GBMs in this study, the *BRAF* mutation has also been detected in E-GBMs that are associated with aggressive clinical behaviors [13, 15]. Indeed, early death after initial treatment was observed in a subset of cases in this study (Case 4), and another cohort including a higher percentage of E-GBMs indicated no survival benefit with a *BRAF* mutation compared with *BRAF*-WT cases [31]. Thus, further molecular biomarkers associated with prognoses should be clarified in *BRAF*-GBMs. Previous reports have revealed frequent combinations of *TERT* promoter mutation both in epithelioid GBMs and classical GBMs with a *BRAF* mutation [13, 15, 16, 29]. In our series, a combination of *BRAF* mutation and *TERT* promoter mutation was detected only in one patient with a classical GBM. Although the *TERT* promoter mutation has been reported as a poor prognosis marker of *IDH*-wild GBMs [32], it is still unclear whether the *TERT* promoter mutation is a prognostic marker in *BRAF*-mutant GBMs. *CDKN2A*-HD has also been detected in a large fraction of *BRAF*-mutant GBMs, which suggests the important role of tumorigenesis in *BRAF*-GBM. However, the diagnostic value of *CDKN2A*-HD in *BRAF*-GBMs is still unclear.

A well-circumscribed border and mild perifocal edema on MRI were frequent in non-hemorrhagic cases in this study and similar findings have been reported in previous studies [9, 29, 33]. However, a recent study suggested that a combination of well-circumscribed borders, large cysts, and cortical involvement was more definitive in *BRAF*-mutant cases rather than the extent of perifocal edemas [31]. Although one patient in our study had multifocal lesions and cases with diagnosis of gliomatosis cerebri harboring a *BRAF* mutation have been reported [6, 29, 34], the majority of *BRAF*-GBMs show a single lesion on MRI [9, 20, 22, 25, 29, 31].

In our series, a prior lesion and hemorrhagic onset were observed in two and three cases, respectively, both of which have not been reported as characteristics of *BRAF*-GBM previously. Prior lesions would suggest the presence of

low-grade pathology, which supports the hypothesis that a subset of *BRAF*-GBMs arise from low-grade *BRAF*-associated tumors, such as PXA [35, 36]. Hemorrhagic onset is a rare clinical presentation in GBMs and several underlying mechanisms such as perivascular necrosis with subsequent loss of vessel support, thin walled or poorly formed vessels, endothelial proliferation with subsequent obliteration of the lumen, and the presence of intratumoral arteriovenous fistulae have been reported [37]. Among previous cases with *BRAF*-GBM, one patient with hemorrhagic onset has been reported [38]. Although the specific mechanism of hemorrhage associated with the *BRAF* mutation is unclear in pathological and radiological examinations in our cases, considering the frequency in this study, hemorrhagic onset may be frequent in *BRAF*-GBM cases.

Conclusions

Analysis of *BRAF* in GBM cases is recommended, especially in patients younger than 55 years of age and *IDH1*-R132 negative cases. Considering the clinical course, a prior lesion and hemorrhagic onset suggest the possible presence of a *BRAF* mutation.

Acknowledgments:

The authors would like to thank Enago (www.enago.jp) for the English language review.

Conflict of interest

The authors declare that they have no conflict of interest.

References

1. Louis DN, Perry A, Reifenberger G et al. (2016) The 2016 World Health Organization Classification of Tumors of the Central Nervous System: a summary. Acta neuropathologica 131:803-820
2. Louis DN, Perry A, Wesseling P et al. (2021) The 2021 WHO Classification of Tumors of the Central Nervous System: a summary. Neuro-oncology. doi:10.1093/neuonc/noab106
3. Taslimi S, Ye VC, Zadeh G (2021) Lessons learned from contemporary glioblastoma randomized clinical trials through systematic review and network meta-analysis: part 2 newly diagnosed disease. Neurooncol Adv 3:vdab028
4. Chappe C, Padovani L, Scavarda D et al. (2013) Dysembryoplastic neuroepithelial tumors share with pleomorphic xanthoastrocytomas and gangliogliomas BRAF(V600E) mutation and expression. Brain Pathol 23:574-583
5. Myung JK, Cho H, Park CK et al. (2012) Analysis of the BRAF(V600E) Mutation in Central Nervous System Tumors. Transl Oncol 5:430-436
6. Schindler G, Capper D, Meyer J et al. (2011) Analysis of BRAF V600E mutation in 1,320 nervous system tumors reveals high mutation frequencies in pleomorphic xanthoastrocytoma, ganglioglioma and extra-cerebellar pilocytic astrocytoma. Acta Neuropathol 121:397-405
7. Lee D, Cho YH, Kang SY et al. (2015) BRAF V600E mutations are frequent in dysembryoplastic neuroepithelial tumors and subependymal giant cell astrocytomas. Journal of surgical oncology 111:359-364

8. Arita H, Yamasaki K, Matsushita Y et al. (2016) A combination of TERT promoter mutation and MGMT methylation status predicts clinically relevant subgroups of newly diagnosed glioblastomas. Acta Neuropathol Commun 4:79
9. Hatae R, Hata N, Suzuki SO et al. (2017) A comprehensive analysis identifies BRAF hotspot mutations associated with gliomas with peculiar epithelial morphology. Neuropathology 37:191-199
10. Park CK, Lee SH, Kim JY et al. (2014) Expression level of hTERT is regulated by somatic mutation and common single nucleotide polymorphism at promoter region in glioblastoma. Oncotarget 5:3399-3407
11. Zhang RQ, Shi Z, Chen H et al. (2016) Biomarker-based prognostic stratification of young adult glioblastoma. Oncotarget 7:5030-5041
12. Kleinschmidt-DeMasters BK, Aisner DL, Birks DK et al. (2013) Epithelioid GBMs show a high percentage of BRAF V600E mutation. Am J Surg Pathol 37:685-698
13. Sun K, Zhou X, Li T et al. (2021) Clinicopathological characteristics and treatment outcomes of epithelioid glioblastoma. Neurosurg Rev. doi:10.1007/s10143-021-01492-7
14. Louis DN, Giannini C, Perry A et al. (2021) Glioblastoma, IDH-wildtype. In: WHO Classification of Central nervous system tumours [Internet], 5th edn. International Agency for Research on Cancer, Lyon (France). Available from: https://tumourclassification.iarc.who.int/chapters/45
15. Nakajima N, Nobusawa S, Nakata S et al. (2017) BRAF V600E, TERT promoter mutations and CDKN2A/B homozygous deletions are frequent in epithelioid glioblastomas: a histological and molecular analysis focusing on intratumoral heterogeneity. Brain Pathol. doi:10.1111/bpa.12572
16. Dono A, Vu J, Anapolsky M et al. (2020) Additional genetic alterations in BRAF-mutant gliomas correlate with histologic diagnoses. J Neurooncol 149:463-472
17. Johanns TM, Ferguson CJ, Grierson PM et al. (2018) Rapid Clinical and Radiographic Response With Combined Dabrafenib and Trametinib in Adults With BRAF-Mutated High-Grade Glioma. J Natl Compr Canc Netw 16:4-10
18. Kaley T, Touat M, Subbiah V et al. (2018) BRAF Inhibition in BRAF(V600)-Mutant Gliomas: Results From the VE-BASKET Study. Journal of clinical oncology : official journal of the American Society of Clinical Oncology 36:3477-3484
19. Kanemaru Y, Natsumeda M, Okada M et al. (2019) Dramatic response of BRAF V600E-mutant epithelioid glioblastoma to combination therapy with BRAF and MEK inhibitor: establishment and xenograft of a cell line to predict clinical efficacy. Acta Neuropathol Commun 7:119
20. Kushnirsky M, Feun LG, Gultekin SH et al. (2020) Prolonged Complete Response With Combined Dabrafenib and Trametinib After BRAF Inhibitor Failure in BRAF-Mutant Glioblastoma. JCO Precis Oncol 4
21. Lin Z, Xu H, Yang R et al. (2021) Effective treatment of a BRAF V600E-mutant epithelioid glioblastoma patient by vemurafenib: a case report. Anticancer Drugs. doi:10.1097/cad.0000000000001130
22. Qin C, Long W, Zhang C et al. (2020) Multidisciplinary Therapy Managed Recurrent Glioblastoma in a BRAF-V600E Mutant Pregnant Female: A Case Report and Review of the Literature. Front Oncol 10:522816
23. Robinson GW, Orr BA, Gajjar A (2014) Complete clinical regression of a BRAF V600E-mutant pediatric glioblastoma multiforme after BRAF inhibitor therapy. BMC Cancer 14:258
24. Venkatesh A, Joshi A, Allinson K et al. (2021) Response to BRAF and MEK1/2 inhibition in a young adult with BRAF V600E mutant epithelioid glioblastoma multiforme: A Case Report and Literature Review. Curr Probl Cancer. doi:10.1016/j.currproblcancer.2020.100701:100701
25. Woo PYM, Lam TC, Pu JKS et al. (2019) Regression of BRAF (V600E) mutant adult glioblastoma after primary combined BRAF-MEK inhibitor targeted therapy: a report of two cases. Oncotarget 10:3818-3826
26. Ebi H, Bando H (2019) Precision Oncology and the Universal Health Coverage System in Japan. JCO Precis Oncol 3
27. Louis DN, Ohgaki H, D.Wiestler O et al. (2016) WHO Classification of Tumours of the Central Nervous System. Revised 4th edition Edition. International Agency for Research on Cancer, Lyon
28. Ishi Y, Takamiya S, Seki T et al. (2020) Prognostic role of H3K27M mutation, histone H3K27 methylation status, and EZH2 expression in diffuse spinal cord gliomas. Brain tumor pathology. doi:10.1007/s10014-020-00369-9
29. Lim-Fat MJ, Song KW, Iorgulescu JB et al. (2021) Clinical, radiological and genomic features and targeted therapy in BRAF V600E mutant adult glioblastoma. J Neurooncol 152:515-522
30. McNulty SN, Schwetye KE, Ferguson C et al. (2021) BRAF mutations may identify a clinically distinct subset of glioblastoma. Sci Rep 11:19999
31. Natsumeda M, Chang M, Gabdulkhaev R et al. (2021) Predicting BRAF V600E mutation in glioblastoma: utility of radiographic features. Brain tumor pathology. doi:10.1007/s10014-021-00407-0
32. Nonoguchi N, Ohta T, Oh JE et al. (2013) TERT promoter mutations in primary and secondary glioblastomas. Acta neuropathologica 126:931-937
33. Suzuki Y, Takahashi-Fujigasaki J, Akasaki Y et al. (2015) BRAF V600E-mutated diffuse glioma in an adult

patient: a case report and review. Brain tumor pathology. doi:10.1007/s10014-015-0234-4
34. Fernandez-Vega I, Quirk J, Norwood FL et al. (2014) Gliomatosis cerebri type 1 with extensive involvement of the spinal cord and BRAF V600E mutation. Pathol Oncol Res 20:215-220
35. Tanaka S, Nakada M, Nobusawa S et al. (2014) Epithelioid glioblastoma arising from pleomorphic xanthoastrocytoma with the BRAF V600E mutation. Brain tumor pathology 31:172-176
36. Watanabe N, Ishikawa E, Kohzuki H et al. (2020) Malignant transformation of pleomorphic xanthoastrocytoma and differential diagnosis: case report. BMC Neurol 20:21
37. Joseph DM, O'Neill AH, Chandra RV et al. (2017) Glioblastoma presenting as spontaneous intracranial haemorrhage: Case report and review of the literature. J Clin Neurosci 40:1-5
38. Chi AS, Batchelor TT, Yang D et al. (2013) BRAF V600E mutation identifies a subset of low-grade diffusely infiltrating gliomas in adults. Journal of clinical oncology : official journal of the American Society of Clinical Oncology 31:e233-236

Figure legends

Fig. 1 Patient demographics and clinical features of a GBM with a *BRAF* mutation in this study

a Genetic landscape presenting mutations of *BRAF*, *IDH1/2,* and *TERT* promoters in nine cases (5.0%), nine cases (5.0%), and 96 cases (54.9%), respectively.

b Age at onset [median (range)] in the BRAF group, IDH group, and WT group was 37 (27–66) years, 43 (22–67) and 63 (15–89) years, respectively. Age at onset in the BRAF group and IDH group was significantly younger than in the WT group ($p = 0.0005$ and $p = 0.0151$, respectively). ANOVA: *; $p < 0.05$, ***; $p < 0.001$

c Among 46 cases with negative IDH1-R132H staining and age <55 years, a *BRAF* mutation was detected in seven cases (15.2%) and no cases harbored an *IDH1/2* mutation.

d Kaplan-Meier survival curve in this study presenting significantly longer OS for the BRAF group and IDH group compared with the WT group ($p = 0.0364$ and $p = 0.0162$, respectively). CI = confidence interval; HR = hazard ratio

Fig. 2 Radiological and pathological findings of representative cases with non-hemorrhagic onset (A–C: case 1, D–F: case 4)

a Preoperative Gd-T1WI of MRI of case 1 who had a tumor with ring-like enhancement in the left mesial temporal lobe.

b HE staining of case 1 (original magnification 4×, scale bar = 200 μm) showing global necrosis.

c HE staining of case 1 (original magnification 20×, scale bar = 50 μm) showing dense tumor cells with nuclear atypia.

d Preoperative Gd-T1WI of MRI of case 4 who had a tumor with ring-like enhancement in the right frontal lobe.

e HE staining of case 4 (original magnification 4×, scale bar = 200 μm) showing global necrosis and microvascular proliferation.

f HE staining of case 4 (original magnification 40×, scale bar = 20 μm) showing dense tumor cells with nuclear atypia with gemistocytic tumor cells supporting the diagnosis of E-GBM.

Fig. 3 Radiological and pathological findings of a representative case with hemorrhagic onset (Case 7)

a Radiological findings at presentation (left: CT, right: FLAIR) indicating a high-density lesion in the left insular cortex

and high intensity lesion surrounding the hemorrhage.

b HE staining (original magnification 20 ×, scale bar = 50 μm) showing diffusely proliferating astrocytic tumor cells with a prominent eosinophilic cytoplasm and multinucleated giant cells and occasional microcalcification.

c Postoperative FLAIR of MRI indicating removal of the right putaminal hemorrhage.

d Gd-T1WI of MRI taken at nine months after the initial surgery indicating the recurrence of a ring-like enhanced lesion.

e HE staining (original magnification 20×, scale bar = 50 μm) showing dense pleomorphic tumor cells with nuclear atypia.

Fig. 4 Radiological and pathological findings of representative cases with a prior lesion and hemorrhagic onset (a–c: case 8, d–f: case 9)

a FLAIR of case 8 taken at the age of 28 years showing a high intensity lesion in the right occipital lobe.

b Radiological findings of case 8 at 31 years of age (left: CT, middle FLAIR, right: Gd-T1WI) showing a high-density lesion with hemorrhage surrounding a high intensity lesion and heterogeneous enhancement in the wall of the lesion in the right occipital lobe.

c HE staining of case 8 (original magnification 10×, scale bar = 100 μm) showing highly cellular tumor cells with palisading necrosis.

d FLAIR of case 9 taken at the age of 30 years showing a high intensity lesion in the right temporal lobe.

e Radiological findings of case 9 at 31 years of age (left: CT, right: FLAIR) showing a high-density lesion with hemorrhage and a surrounding high intensity lesion in the right temporal lobe.

f HE staining (original magnification 40×, scale bar = 20 μm) indicating astrocytic tumor cells with a monomorphic population.

Table. Summary of BRAF-GBM in this study

Case	Age at onset (years)	Gender	Initial symptom	Location	Prior lesion	Pathological diagnosis	*BRAF*	*IDH1/2*	*TERT*	*CDKN2A*	Recurrence	OS (months)	Status
1	27	F	Seizure	Temporal lobe	Unknown	GBM	V600E	WT	WT	HD	−	77	A
2	37	M	Seizure	Parietal lobe	Unknown	GBM	V600E	WT	WT	HD	−	38	A
3	37	M	Verbal abnormality	Temporal lobe	Unknown	GBM	V600E	WT	WT	HD	+ Dis	84	D
4	42	M	Seizure	Frontal lobe	Unknown	E-GBM	V600E	WT	WT	HD	+ Dis	5	D
5	61	M	Facial numbness	Multifocal	Unknown	GBM	V600E	WT	WT	HD	+	12	D
6	66	M	Consciousness disturbance	Temporal lobe	Unknown	GBM	V600E, K601del	WT	WT	No loss	+ Dis	37	D
7	44	F	Stroke-like (hemorrhagic)	Frontal lobe	Unknown	GBM	V600E	WT	WT	No loss	−	48	A
8	31	M	Stroke-like (hemorrhagic)	Occipital lobe	+ (28-year-old)	GBM	V600E	WT	WT	HD	+ Dis	29	D
9	38	M	Stroke-like (hemorrhagic)	Temporal lobe	+ (30-year-old)	GBM	V600E	WT	C250T	HD	−	30	A

Abbreviations: A = alive; D = dead; Dis = dissemination; E-GBM = epithelioid glioblastoma; F = female; GBM = glioblastoma; HD = homozygous deletion; M = male; OS = overall survival; WT = wild-type

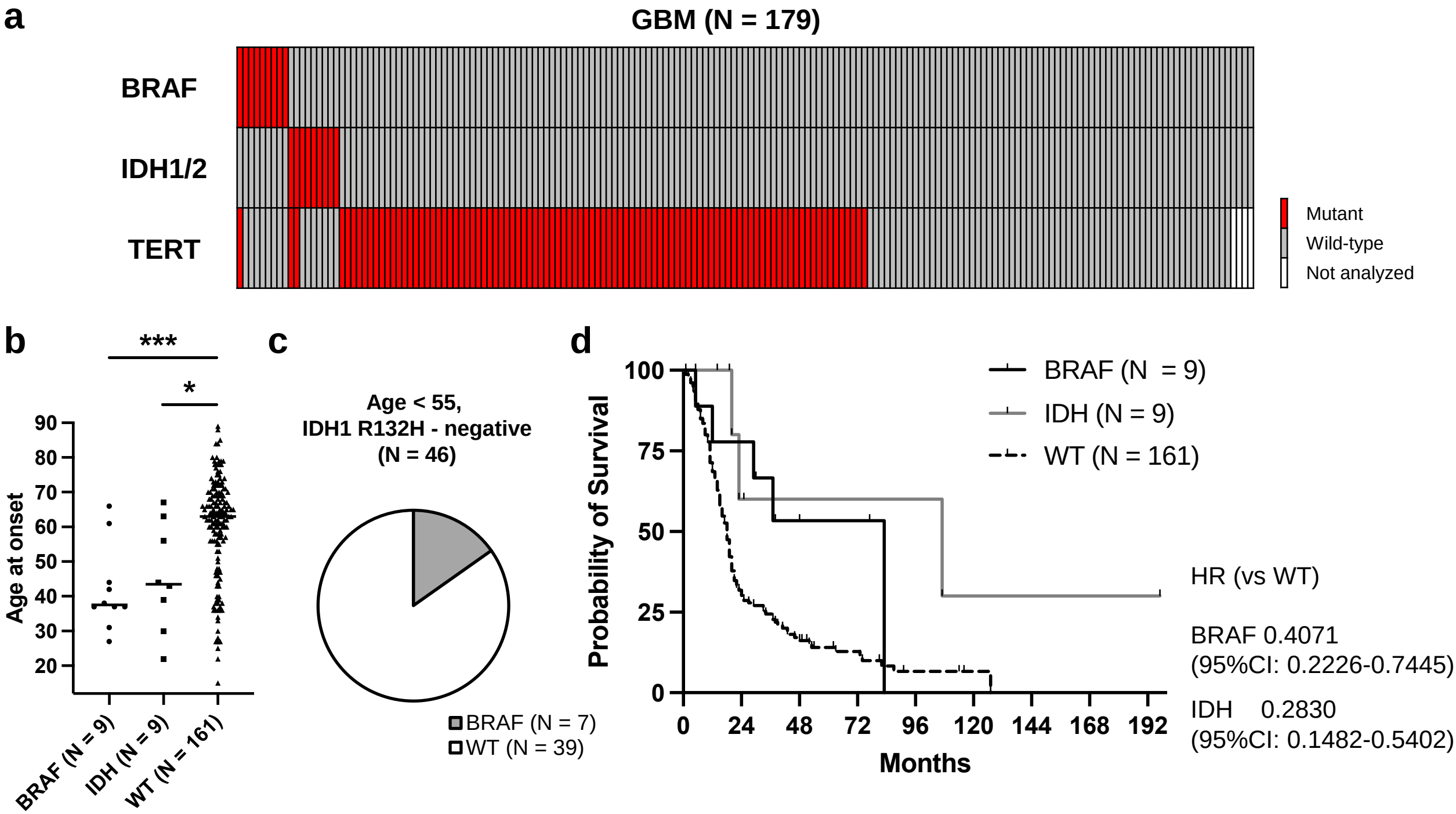
a
GBM (N = 179)
BRAF
IDH1/2
TERT
Mutant
Wild-type
Not analyzed
b
***
*
Age at onset
90
80
70
60
50
40
30
20
BRAF (N = 9)
IDH (N = 9)
WT (N = 161)
c
Age < 55,
IDH1 R132H - negative
(N = 46)
BRAF (N = 7)
WT (N = 39)
d
Probability of Survival
100
75
50
25
0
0
24
48
72
96
120
144
168
192
Months
BRAF (N = 9)
IDH (N = 9)
WT (N = 161)
HR (vs WT)
BRAF 0.4071
(95%CI: 0.2226-0.7445)
IDH 0.2830
(95%CI: 0.1482-0.5402)

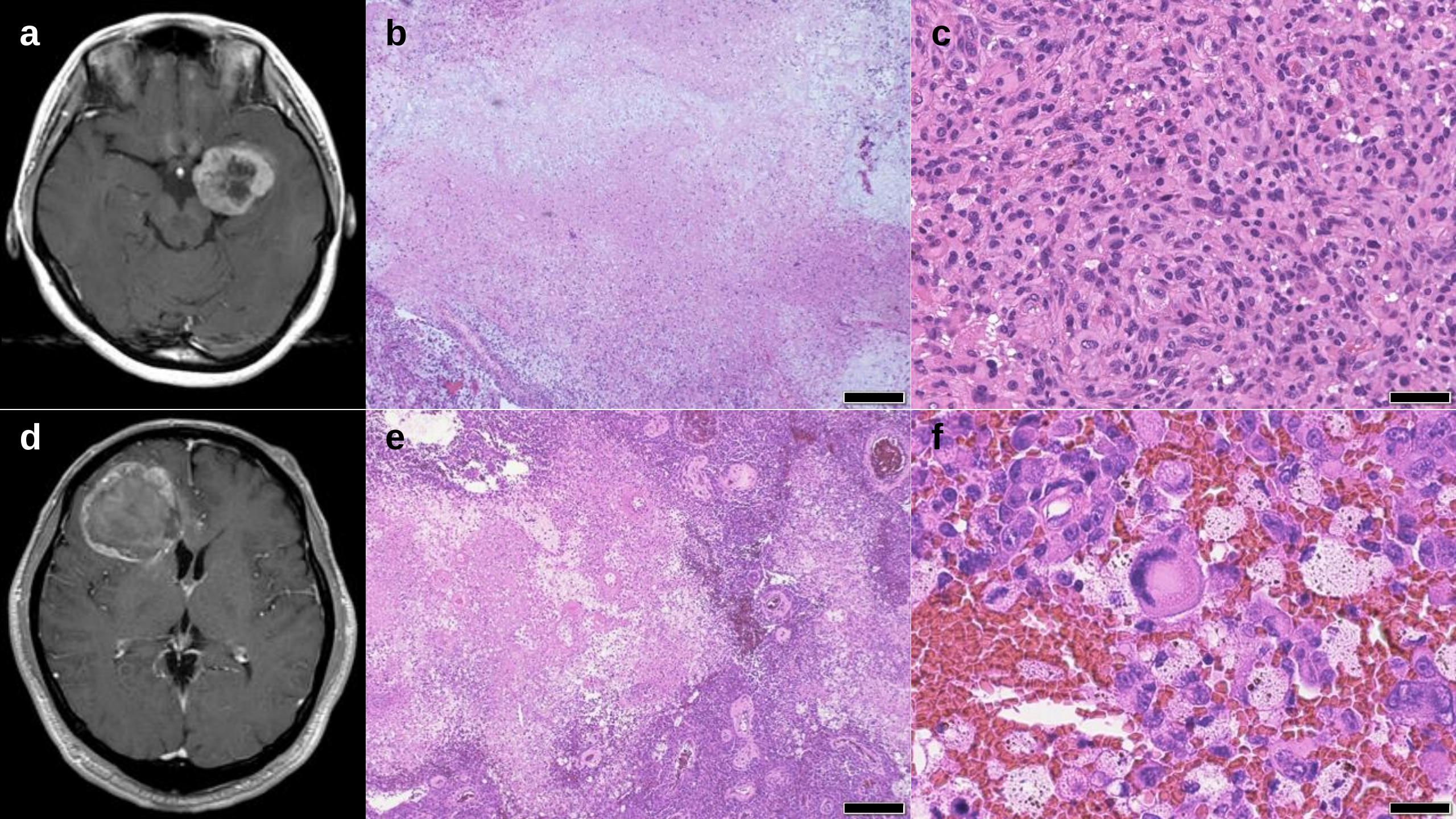
a
b
c
d
e
f

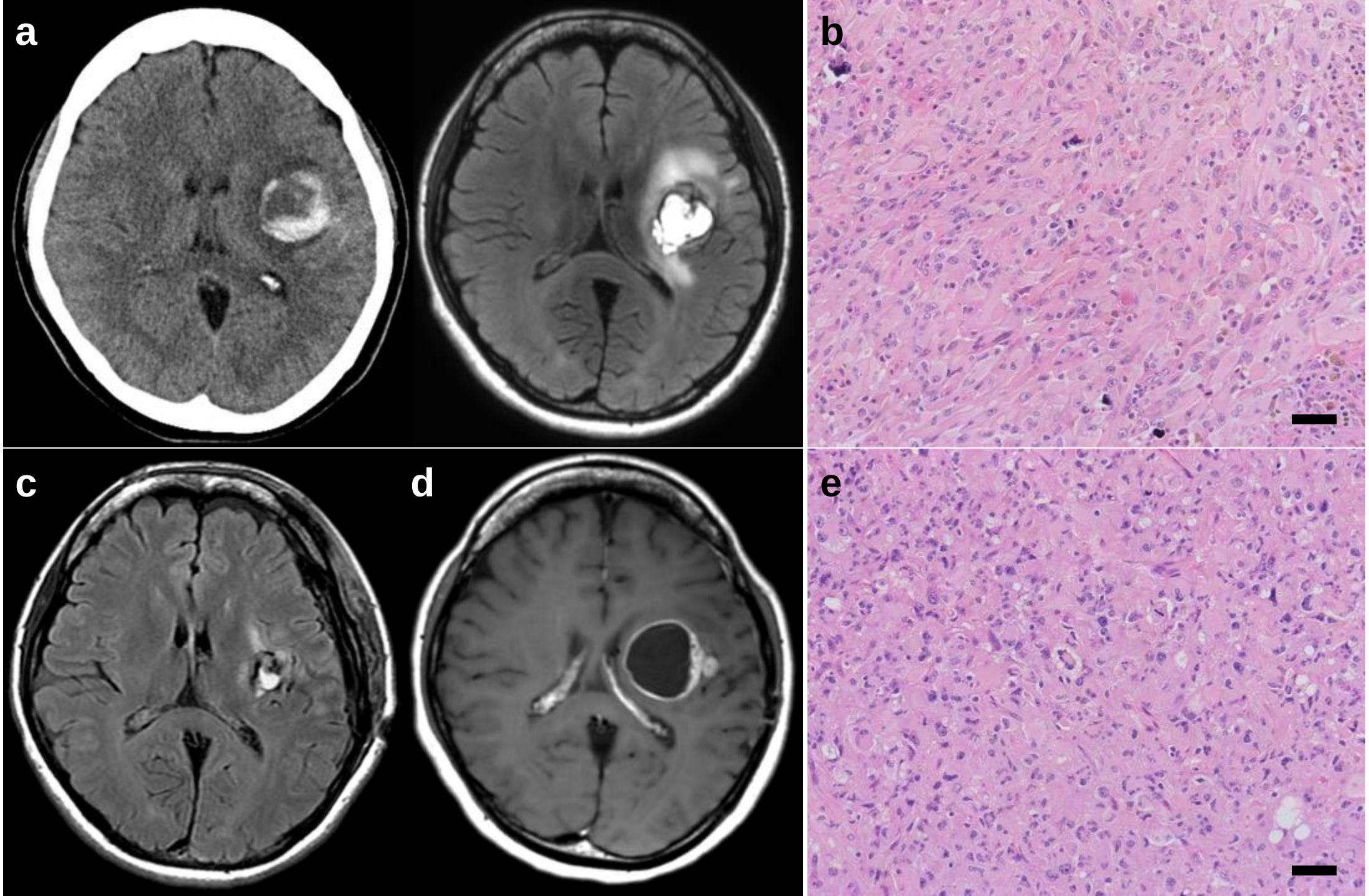
a
b
c
d
e

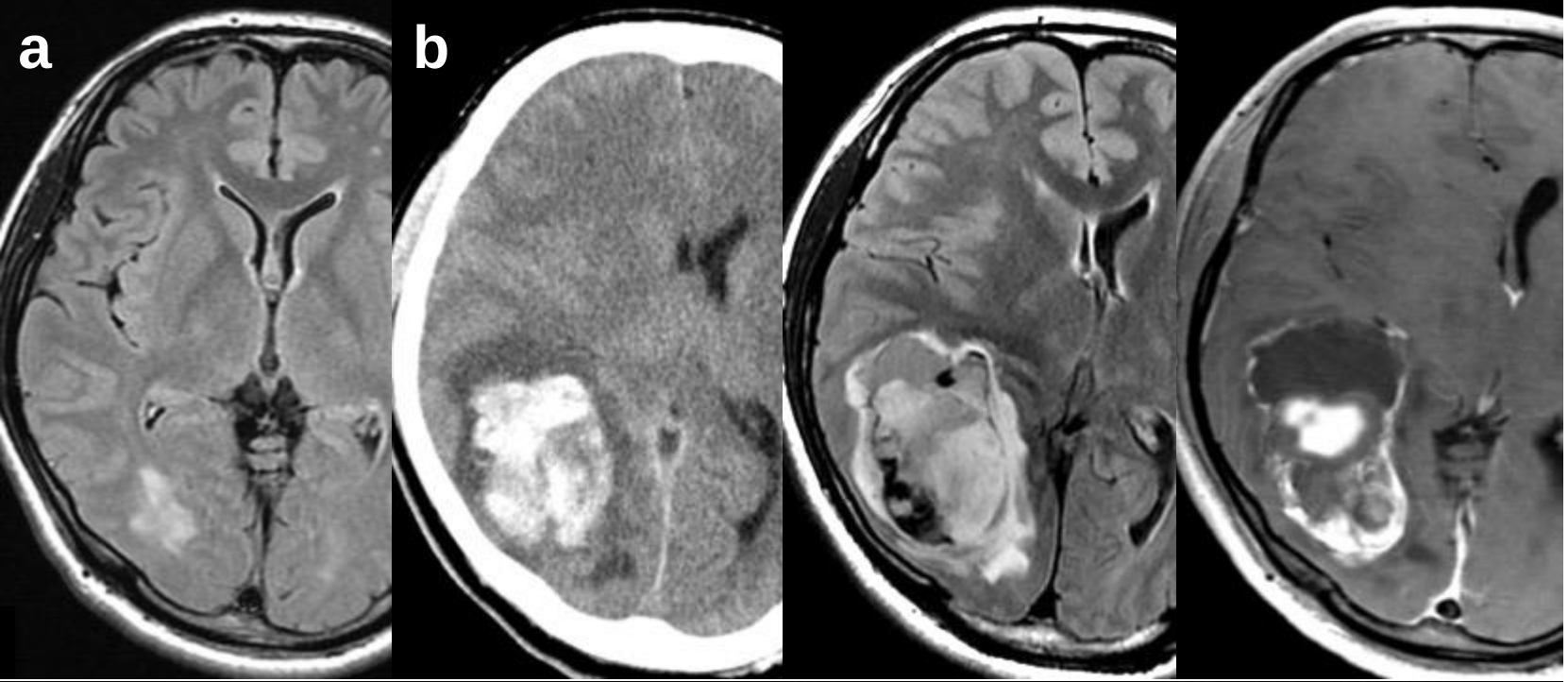
a
b

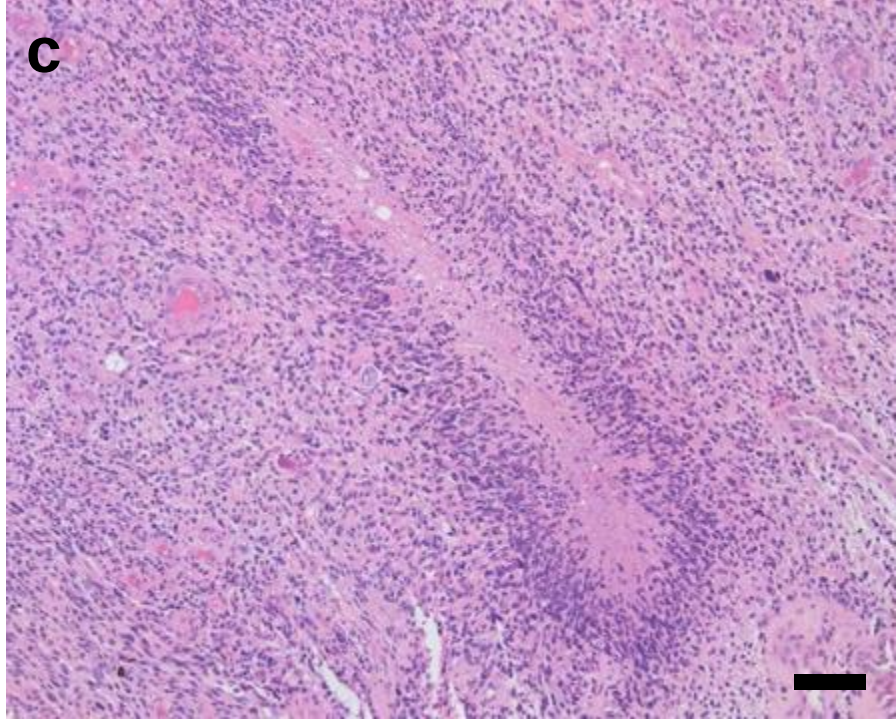
c

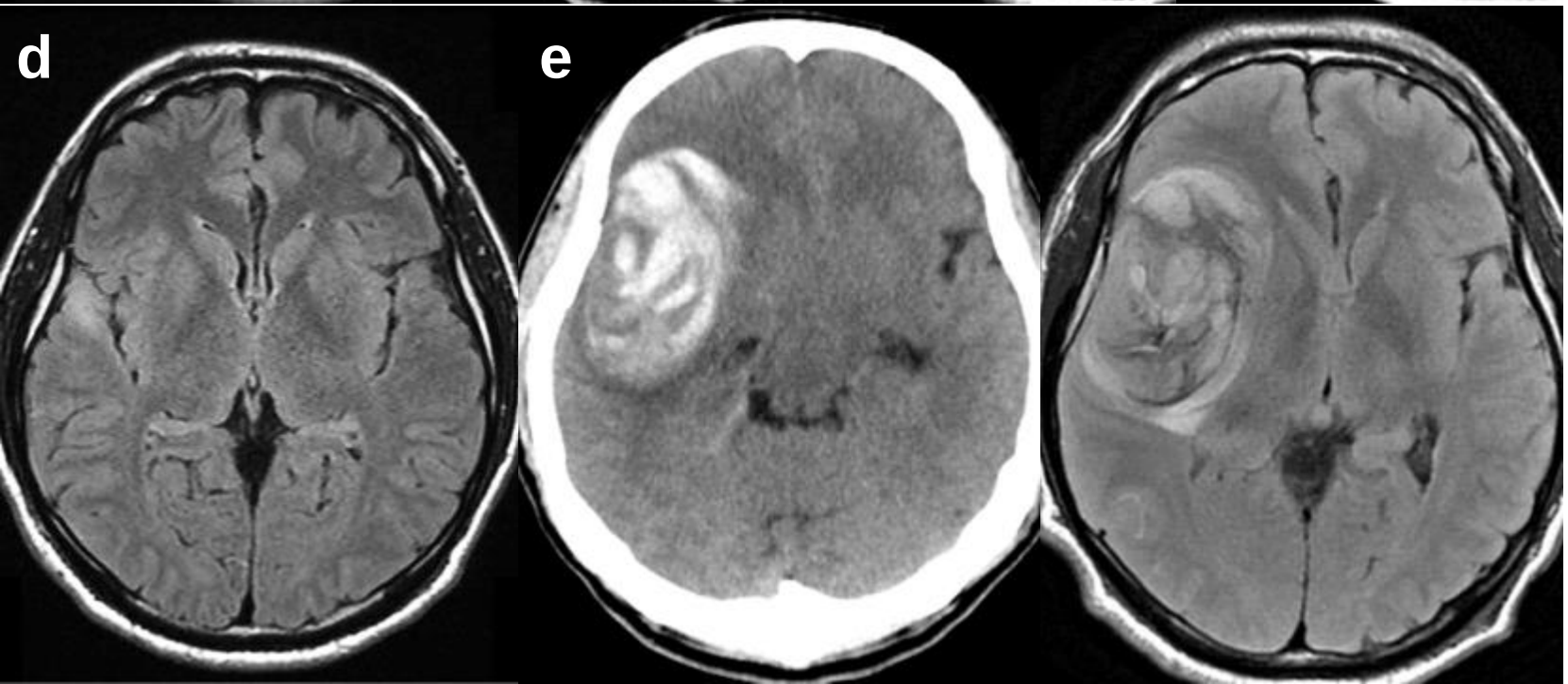
d
e

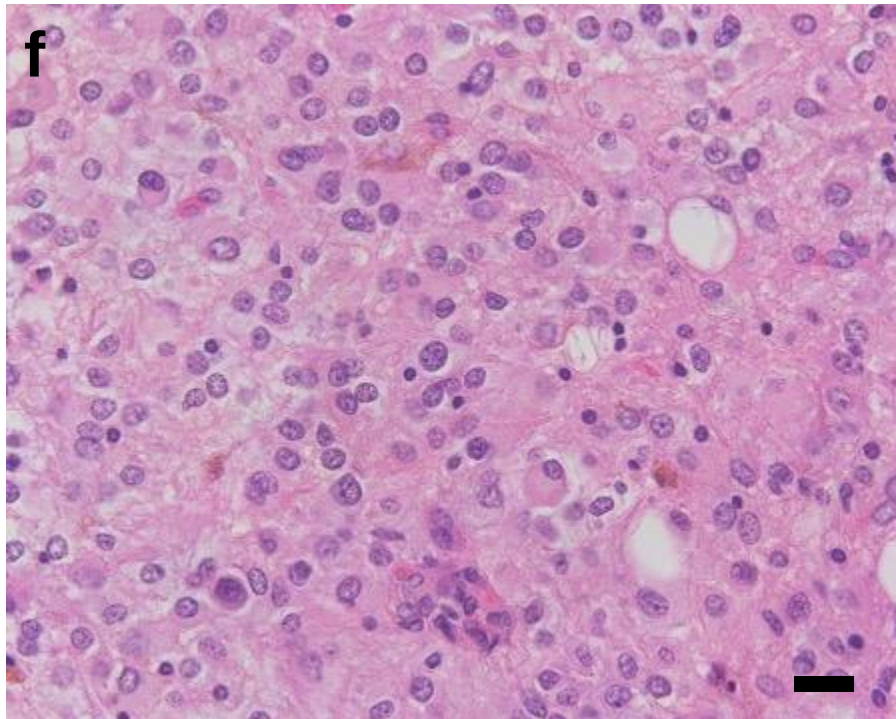
f